Journal of Structural Geology, Vol. 15, No. 8, pp. 949 to 964, 1993
Printed in Great Britain

0191-8141/93 $06.00+0.0

Deformation at the toe of an active accretionary prism: synopsis of results from ODP Leg 131, Nankai, SW Japan

A. J. MALTMAN

Institute of Earth Studies, University College of Wales, Aberystwyth SY23 3DB, U.K.

T. BYRNE

Department of Geology and Geophysics, University of Connecticut, 354 Mansfield Road, Storrs, CT 06269-2045, U.S.A.

D. E. KARIG

Department of Geological Sciences, Cornell University, Ithaca, NY14853-1504, U.S.A.

and

S. LALLEMANT

Laboratoire de Geologie, Ecole Normale Superieure, 24 Rue Lhomond, 75231 Paris Cédex 05, France

(*Received* 13 *March* 1992; *accepted in revised form* 6 *October* 1992)

Abstract—Toes of accretionary prisms record the initial deformation of wet sediments during accretion at a convergent plate margin. ODP Leg 131 succeeded in coring the toe of the Nankai prism, SW Japan, together with the basal décollement, the underthrust sediments and the basaltic ocean basement. An unprecedented structural geological inventory has been compiled. Gravitational deformation is important in the slope-apron deposits, but tectonic stresses, too, are transmitted to these levels. Core-scale deformation bands, due to heterogeneous bulk-shortening of the prism, are exceptionally well-developed at Nankai, and range through kink-bands, shear zones and faults. Anomalous frequencies indicate localized high-strain zones. Stress-inversion analysis gives a principal compression close to the plate convergence vector.

The frontal thrust of the prism is a 26 m thick zone of breccia/scaly fabric, with a 309 m net slip. It may well be currently active, and accommodating almost half of the present convergence strain. The basal décollement, a 19 m thick breccia zone, separates the deforming, overconsolidated sediments of the prism from the virtually undeformed materials below. These are highly underconsolidated and probably overpressured. Anomalous fluid pressures localize several of the prism structures. Unlike some other prisms, drainage of the Nankai prism is dominantly pervasive rather than controlled by major structures.

INTRODUCTION

THE toes of accretionary prisms record the first chapters in the story of convergent plate-margin growth. However, these early processes are difficult to decipher from the eventual on-land exposures, because their effects become successively overprinted during subsequent accretion and uplift. Mountain-belt prisms preserve few clues on how the ocean-floor, water-rich sediments responded to deformation during their burial and lithification, yet these initial stages do much to influence the architecture and dynamics of the plate boundary, particularly where an accretionary prism develops. Against this background, Leg 131 of the Ocean Drilling Program (ODP) recently drilled the toe of the Nankai accretionary prism, SW Japan, where the Philippine Sea plate is converging beneath the Eurasian plate. Reasons for selecting the Nankai prism for investigation and the overall goals of the work are given in Taira *et al.* (1991a, pp. 9–13).

One of the objectives was the elucidation of the structural style and fabrics of the actively deforming sediments, and to this end, for the first time in either Deep Sea Drilling Project (DSDP) or ODP operations, four of the shipboard scientists were designated as Structural Geologists, with responsibility for dealing with any deformation structures encountered during the drilling. In the event, such an abundance of information accrued—probably "the most complete structural geological inventory anywhere in the world's oceans" (Taira *et al.* 1991a, p. 110)—that the data, together with the ensuing laboratory analyses, are becoming dispersed over a number of publications. In addition, because another goal of the drilling was to investigate the interplay between fluid flow and deformation, some of the structural geological results are being incorporated into reports on the hydrogeology of the prism. The purpose of this article, therefore, is to provide a synopsis of the data related to the deformation of the Nankai prism toe, and to note some points of interest to a wider structural geological audience.

Tectonic setting

The Philippine Sea plate (Fig. 1a) is bringing hemipelagic sediments northwestwards, at a rate of about 40

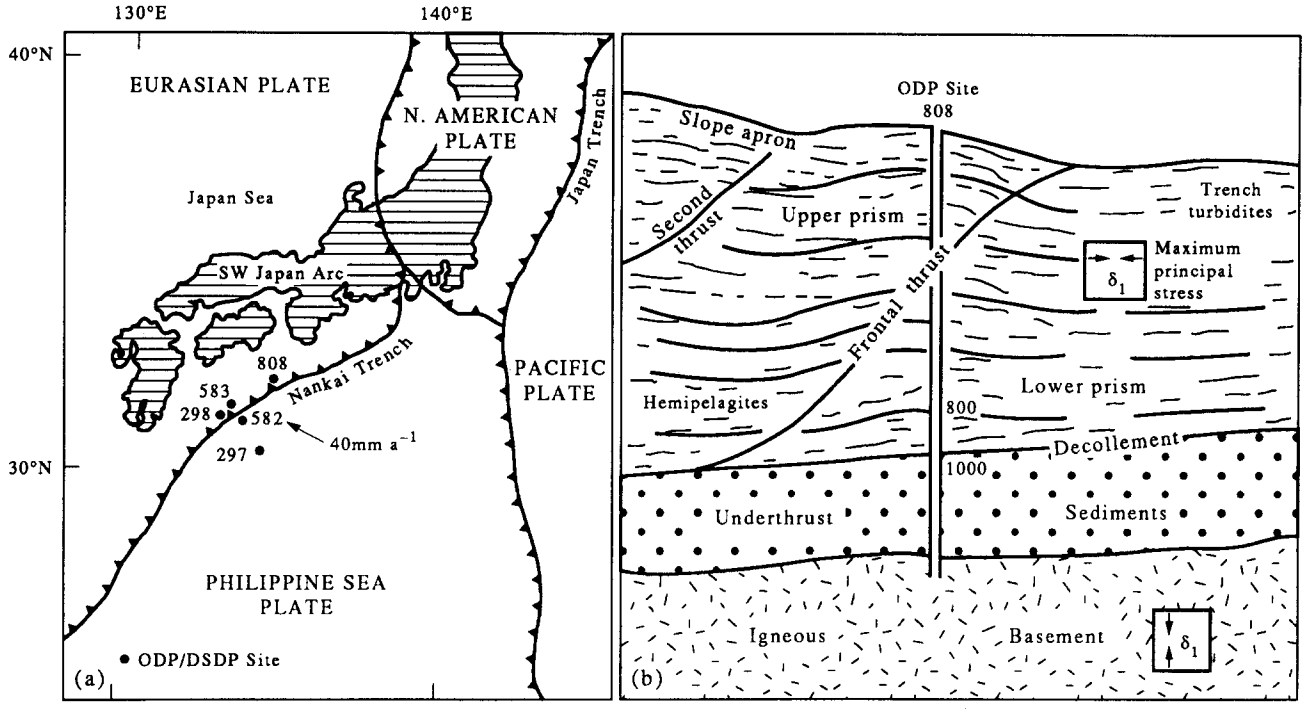

Fig. 1. (a) Map showing the location and plate tectonic setting of Site 808 of ODP Leg 131, and sites of previous drilling. (b) Generalized cross-section showing the main structural elements of the toe region of the Nankai prism penetrated at Site 808.

mm a^{-1}, towards SW Japan, a collage of island arc and earlier accretion systems now part of the Eurasian plate (Taira *et al.* 1989, and references therein). Part of the hemipelagic sequence is being underthrust but the upper part is being offscraped and incorporated into the Nankai prism (Fig. 1b). At the same time, the trench immediately oceanward of the prism, the Nankai Trough, has been receiving large amounts of clastic material from the recently uplifted parts of Japan, and these sediments, too, are being offscraped into the Nankai prism. The accreted and underthrust materials are separated by the basal décollement of the prism. The offscraping process is taking place by the upward and oceanward propagation from the décollement of a series of thrusts, in the general style—very analogous to that of fold-and-thrust belts—now well established for prism growth (e.g. Moore & Lundberg 1986). The overall structure of the Nankai prism toe in the area visited by ODP Leg 131 is apparent from the seismic profiles presented by Moore *et al.* (1990, 1991), and its setting is discussed further by Taira *et al.* (1991a, pp. 273–275). Preliminary results of the drilling were summarized by Taira *et al.* (1991b).

Methodology

The location of the ODP drilling—Site 808—is indicated on Fig. 1. The Pacific Ocean at this point is 4.6 km deep. Also shown on Fig. 1(a) are previous drilling efforts. Sites 297 and 298 were spot-cored during DSDP Leg 31. Sites 582 and 583 were drilled during DSDP Leg 87, the former being a valuable reference hole, having reached a depth of 750 m below the sea floor (mbsf) in the undeformed sediments oceanward of the prism. The latter hole penetrated the prism to 450 mbsf. At Site 808, eight shallow holes were drilled, largely for various down-hole measurements and experiments, together with one hole that cored to a depth of 1327 mbsf. It penetrated the entire accretionary prism—including the frontal thrust zone, the décollement zone, the underthrust hemipelagites, and succeeded in reaching the underlying oceanic basement. With a core recovery rate generally in excess of 50%, it became possible, for the first time ever, to document the variation in structural style throughout the depth of the accreting and underthrusting sediments. Over 3000 shipboard structural measurements were collected and processed. Details of the methods are given in Taira *et al.* (1991a, pp. 39–45). Over 70% of the orientation data were corrected for the rotations that resulted from the rotary drilling. The corrections to true geographic co-ordinates utilized approximately 450 magnetic poles, collected continuously with a pass-through cryogenic magnetometer (Taira *et al.* 1991a, pp. 126–128).

DEFORMATION STRUCTURES SEEN IN THE CORES

Bedding and associated fabrics

Bedding is discernible in many of the cores through fine changes in lithology (Fig. 2). The inclination of much of the bedding reflects the regional orientation expected from the seismic profile, but markedly anomalous steepening occurs near-surface, due to gravitational instabilities, and in two high-strain zones, at about 530 and 800 mbsf. Two zones of dramatic steepening co-

incide exactly with the frontal thrust and the basal décollement. The variable dips in the frontal thrust zone are due to a fold pair associated with the thrusting (Fig. 3), but any such folding in the décollement is now masked by intense brecciation, which seems to be primarily responsible for the steepened bedding in that zone.

Fissility, best developed in cores from deeper levels, results from the alignment of inequant grains parallel to bedding, and is presumably due to gravity-induced consolidation. It is here referred to as a primary sedimentary fabric (psf). It is feeble where the sediment is bioturbated, and as this is particularly common in the hemipelagites, which now form the deeper parts of the prism toe, the increase of the psf with depth is irregular. The intensity of development of the psf appears to be a factor in allowing the production of some of the deformation structures, hence bioturbation also tends to obscure indirectly the distribution of these structures with depth.

There are two lines of evidence for the additional presence in the prism sediments of an unseen penetrative fabric, namely, oriented transverse-sonic velocity measurements (Byrne *et al.* 1991) and low-field magnetic susceptibility data (Owens in preparation). The orientation of the fabric indicates a horizontal NW-shortening of the psf, which is consistent with the plate-convergence vectors. The feature is therefore thought to be recording a component of tectonically-induced consolidation within the prism.

Slump folds

Centimetre-scale reclined and recumbent folds, interpreted as slump structures, occur in the cored slope-

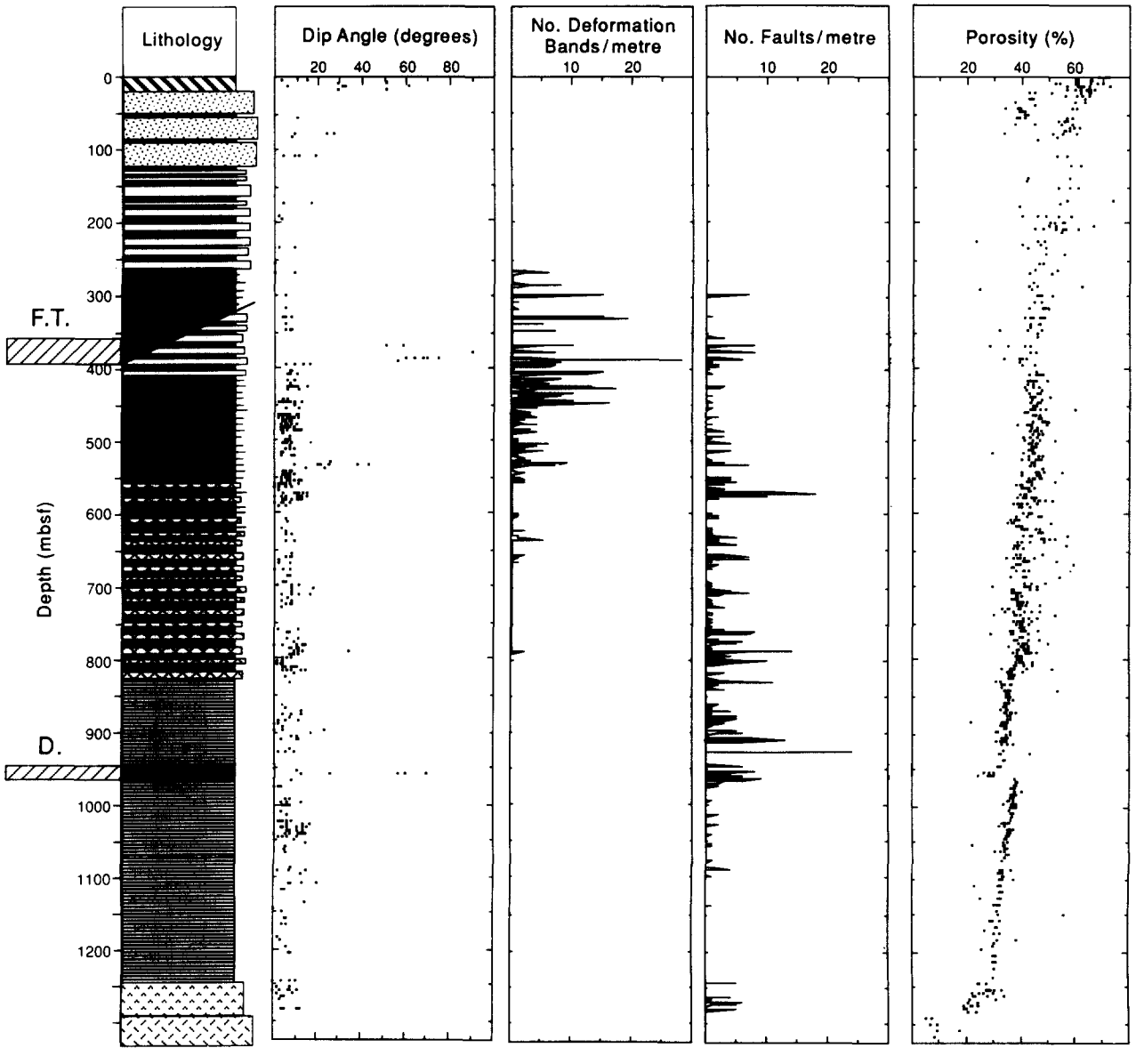

Fig. 2. Distribution with depth of lithology, bedding dips, deformation bands, faults and porosity. The lithological symbols, from top to bottom, are: diagonal stripes = slope apron muds and sands; stipple = sand turbidites; grey tint/white = hemipelagites with thin salt and sand turbidites; pecks = ash/tuff; horizontal rule = hemipelagic mud. The two lowermost units are acid volcaniclastic deposits overlying basaltic basement. F.T. is the frontal thrust zone, and D. the basal décollement zone.

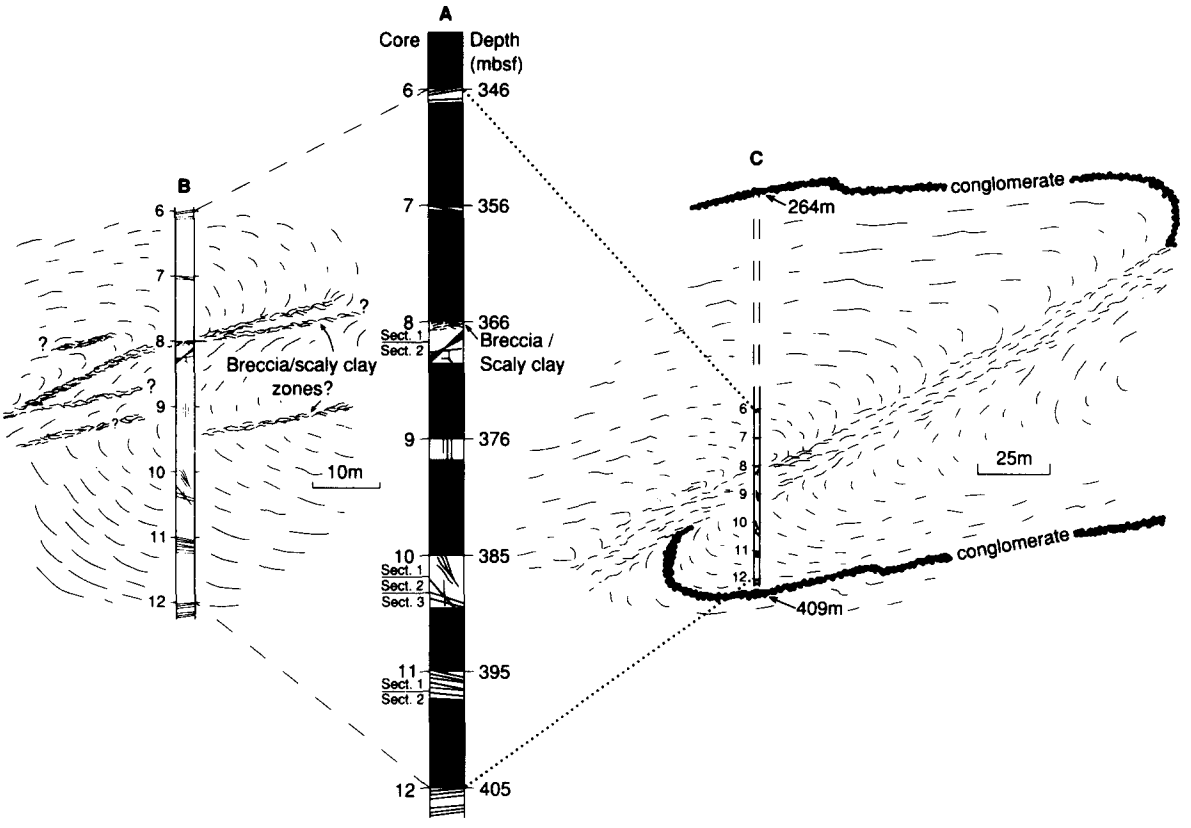

Fig. 3. Interpretation from the recovered cores of the structure of the frontal thrust zone. The core and section numbers follow the O.D.P. convention, explained in Taira *et al.* (1991b).

apron deposits. Together with the near-surface steepening of bedding mentioned above, they testify to the importance of gravitational mass-movements in the toe region of the prism. Seismic profiles show accreted strata removed from the crests of the hangingwall anticlines of the frontal and more landward thrusts, and redeposited lower down the prism and in the trench (Moore *et al.* 1991, p. 19). Hence, the significant proportion of the trench deposits may be recycled material, although it is premature to specify the amounts.

Similar fold structures occur, rarely, deep in the prism, such as at 426 mbsf, considerably below the frontal thrust. A fold closure of similar appearance is also preserved in material from within the décollement zone. These latter examples presumably are legacies of some gravitational instability experienced by the sediment while at or close to the ocean floor. No fabrics have been seen directly associated with any of these structures.

Deformation bands: description

One of the conspicuous features of the Nankai prism is the profusion of core-scale deformation features. The kinds of structures found during DSDP Legs 31 and 87 are also common at Site 808, together with additional types—particularly at the deeper levels of the prism. The contrast in variety and abundance of these structures with those so far reported from other prisms (e.g. Lundberg & Moore 1986) is striking.

These various structures are grouped loosely here under the heading 'deformation bands'. Examples are illustrated in Figs. 4 and 5. They are all roughly planar zones, oblique to bedding, which show some degree of deflection of the psf or other marker. Some examples are sufficiently distinctive to be specified as kink bands, shear zones, or faults, but there are many instances where a particular band shows the characteristics of more than one kind of structure, and is in some ways intermediate in appearance. We refer to such structures as kink-like, shear zone-like or fault-like, according to the dominant attributes. The terminological difficulties are discussed further by Maltman *et al.* (in press). Characteristics of the main types are as follows.

Kink-like deformation bands are common at Nankai. They are 0.5–3 mm wide planar bands, slightly darker than the host sediment, that sharply deflect laminations or the psf (Figs. 4b and 5a) (also Lundberg & Karig 1986). Some are curviplanar and show variable width and some sub-structure, thus resembling shear zones. The most common situation is for a kink-like structure with a degree of sub-structure to be spatially associated with, and at a high angle to, a shallow-dipping shear zone (Figs. 4b and 6). All kink-like bands where deflection is discernible show a reverse sense of movement. Most core-scale kinks strike NE and fall statistically into a conjugate set centred on bedding, with a 30–45° dihedral angle (Fig. 7). It is interesting to note that apart from a remark by Lundberg & Moore (1986) on the Aleutian Trench, all the examples of kink bands so far documented in oceanic sediments come from Nankai.

Leg 131 recovered numerous structures that have

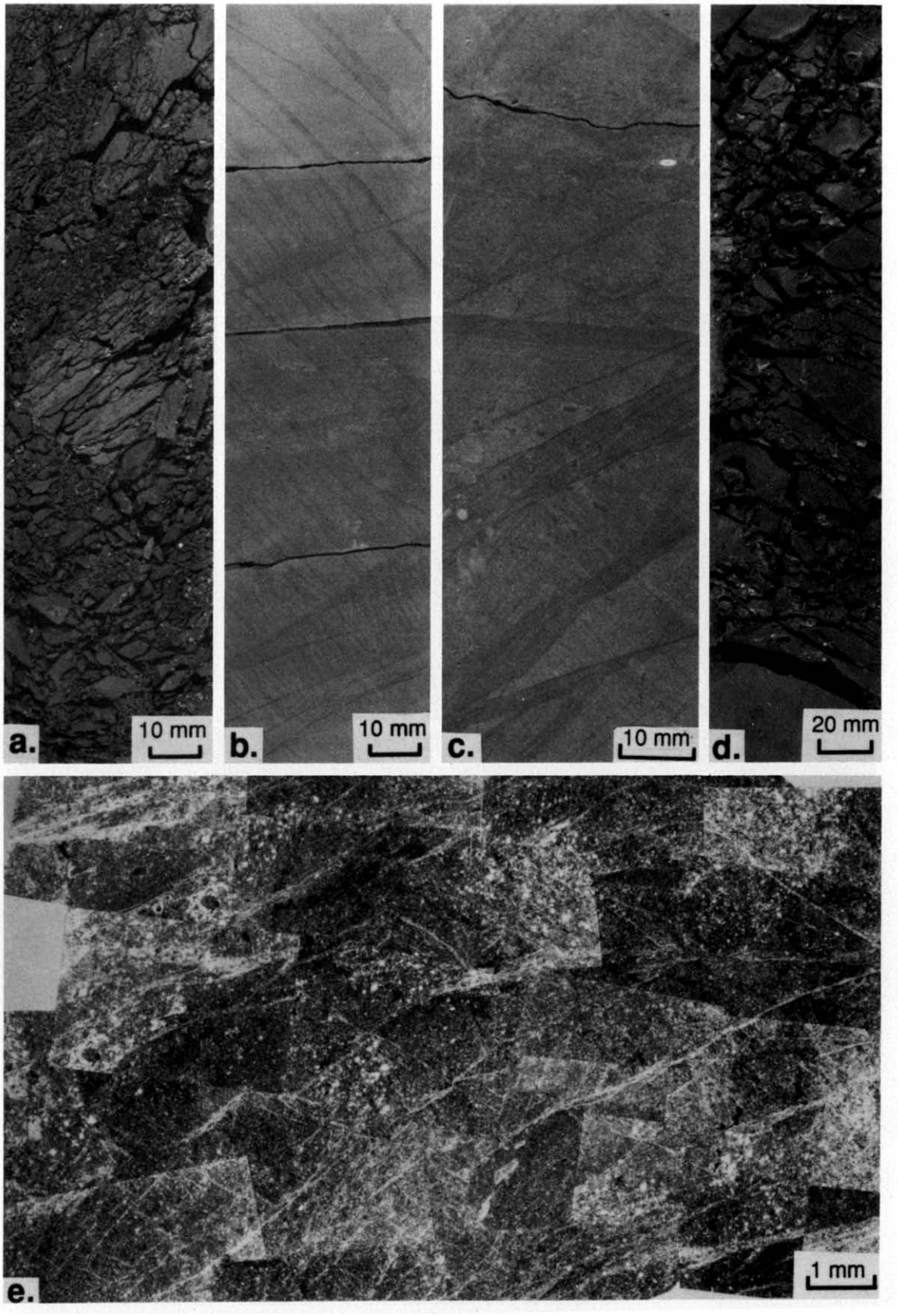

Fig. 4. Typical appearance of structures in the cores. (a) Core photograph of breccia/scaly fabric from the frontal thrust zone. Bedding dips to the left. 365 mbsf. (b) Core photograph of kink-like deformation bands at a high angle to narrower, low-angle shear zone-like bands. 440 mbsf. (c) Core photograph of fault-like (lower angle) and shear zone-like bands. 450 mbsf. (d) Core photograph of breccia from the basal décollement. 960 mbsf. (e) Photomicrograph showing complex fault array. Crossed-polars. 530 mbsf.

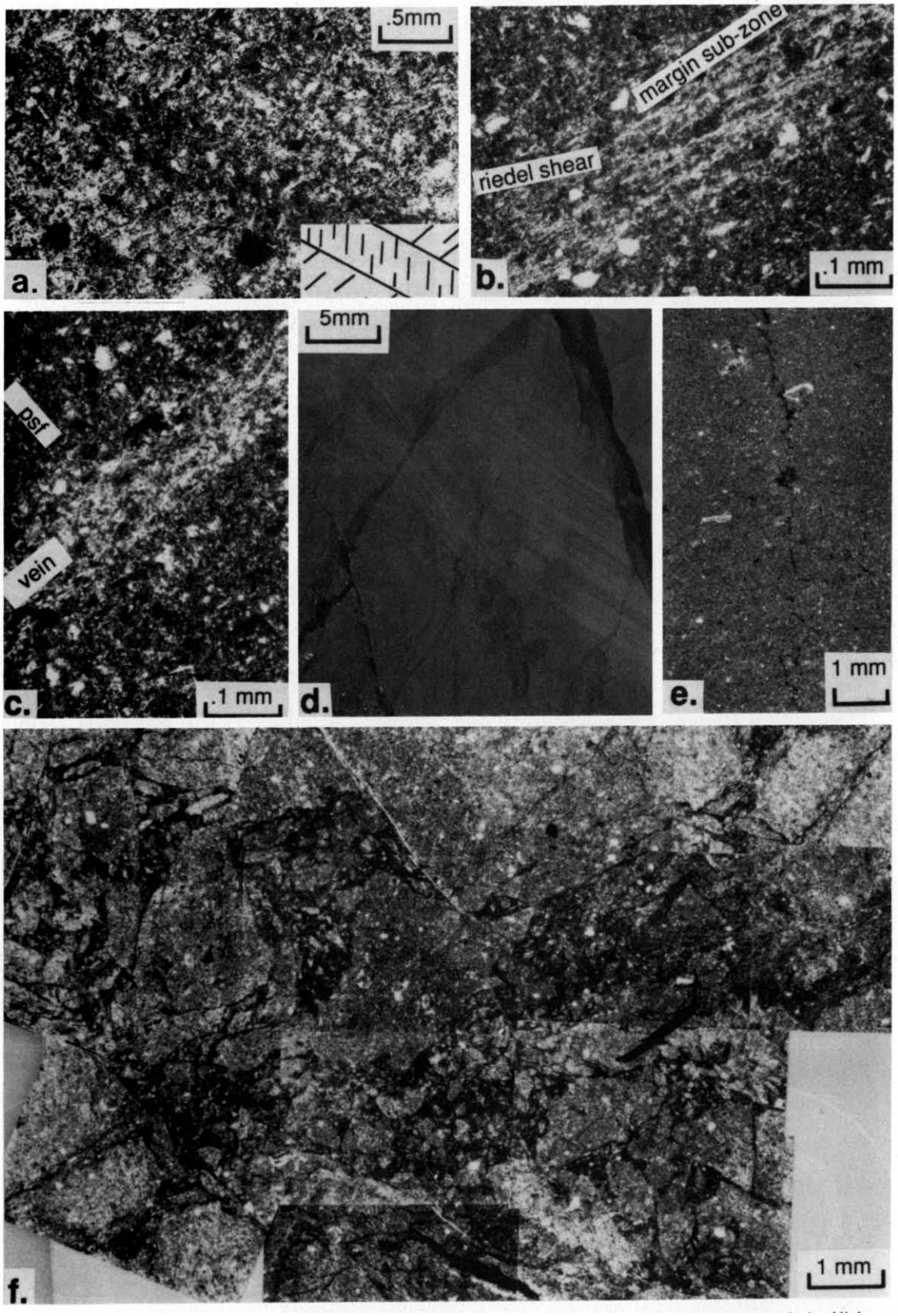

Fig. 5. Aspects of the deformation structures. (a) Detail of kink band, showing lack of sub-structure. Plane-polarized light. 435 mbsf. (b) Detail of shear zone, showing examples of sub-structure. Crossed-polars. 390 mbsf. (c) Detail of vein structure. Crossed-polars. 640 mbsf. (d) Detail at the core scale of irregular faults in the frontal thrust zone. 368 mbsf. (e) Vertical stylolite. Plane-polarized light. 1280 mbsf. (f) Photomicrograph showing patches of 'hydraulic breccia'. Crossed-polars. 788 mbsf.

much in common with the shear zones well known from other deformed sediments (e.g. Maltman 1988, Mandl 1988, pp. 75–80). They are narrower than the kinks described above, have a more irregular and complex geometry, and show an intricate substructure (Fig. 6). Macroscopically, they appear as dark, narrow, commonly anastomosing traces (Fig. 4b). Viewed between crossed polars, the narrow, sharply-bounded zones of intense fabric reorientation show brightly against the darkened host material, and with a one-wavelength accessory plate a range of substructures is apparent (Fig. 5b). In a number of respects, these observations differ from the structures reported from Site 583 by Karig & Lundberg (1990), presumably because a greater range of deformation conditions were encountered at Site 808.

The difficulty of distinguishing between sub-shears in the Riedel and thrust orientations (R_1 and P in sheared rock terminology, e.g. see Shimamoto 1989) makes interpretation of the movement sense ambiguous in the absence of displaced markers. Coalesced arrays of numerous shear zones, and individual very narrow zones that show significantly displaced markers, both approach faults in appearance.

Fault-like deformation bands are characterized by their relative narrowness and the significant displacement along them. Some examples are roughly planar and resemble very narrow shear zones (Figs. 4c & e): a typical microscopic appearance is very similar to the example from the Japan Trench illustrated by Knipe (1986b, fig. 12). Other types, especially in high-strain zones such as the frontal thrust and the décollement, are highly irregular and reach widths of over 1 mm (Fig. 4d). Displacements along them can exceed several centimetres; they are considerably dark or even black in colour. The surfaces are commonly coated with shiny dark material enriched in griegite and/or pyrite, and show stepped, fine grooves or slickenlines. Although microscopically these structures show some features in common with shear zones (Fig. 8), macroscopically they are clearly distinguishable as faults. In the statistical treatment of Fig. 2, for example, they are plotted separately from other deformation bands.

The orientation of the fault structures is more complex than the other deformation bands. Many examples have a shallow dip but very variable strike, producing a gently-inclined web of intersecting faults, but a moderately-dipping conjugate array about bedding is also common (Fig. 9). The structures variously show reverse, normal and strike-slip movement senses. Lallemant *et al.* (in preparation) discuss the various fault geometries in more detail.

Origin of the deformation bands

Stress-tensor analysis based on the lineated surfaces of the deformation bands (Lallemant *et al.* in preparation) demonstrates unequivocally that these structures are tectonically induced—a direct consequence of prism shortening through plate convergence.

Isolated kink bands, normally at a high angle to bedding, and formed only where a significant psf exists, represent a response of anisotropic sediments to bulk sub-horizontal shortening of the prism. Most kink-like bands are spatially related to shear zones, and because some examples are intermediate in appearance, it is tempting to think that increasing displacement enables kinks to evolve into shears. While this may happen in some cases, the two structures are thought normally to originate together. The mutual cross-cutting indicates synchroneity, with the kinks recording the accommodational strains that arise from the principal displacement along the shear zone.

This suggestion is supported by laboratory deformation studies, where identical microstructures, in the same geometrical relationship, form in the constant bulk mechanical conditions of a single experiment (Maltman 1978). The geometry is more commonly developed in bulk simple shear experiments than in triaxial tests. Why a kink geometry is favoured by the steeply oriented movements is unclear: perhaps it is an effect of different strain rates operating in different directions. It is possible that the macroscopic shear zones bear an R_1 orientation to which the kinks are antithetic (R_2, with the microscopic sub-structures representing a lower hierarchy of shear structures (cf. Karig & Lundberg 1990).

These kinds of deformation bands are most common in the upper levels of the Nankai prism, particularly between about 260 and 600 mbsf (porosities between 45

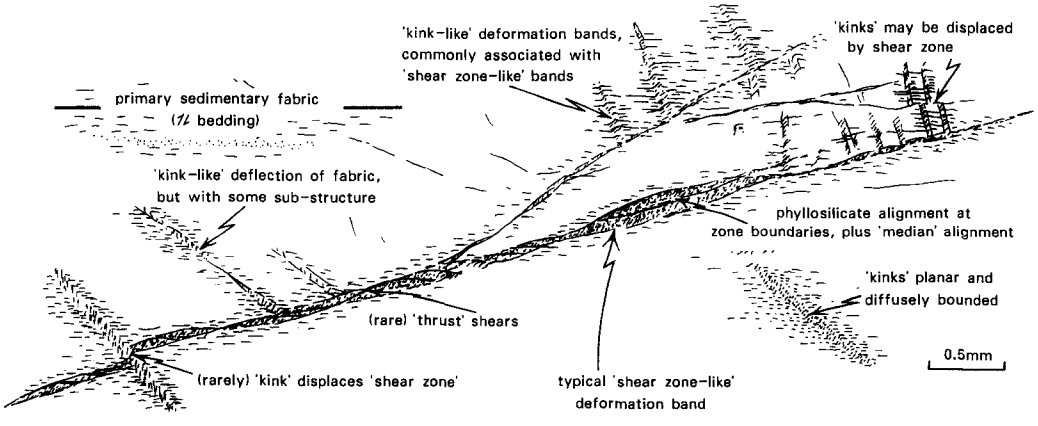

Fig. 6. Sketch of typical features of shear zones when viewed at the optical microscope scale.

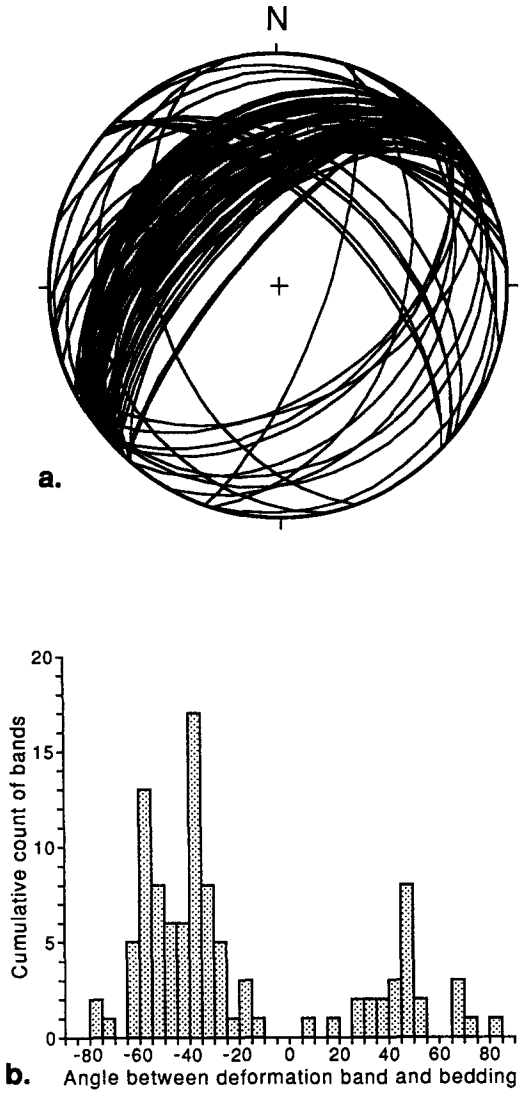

Fig. 7. Orientation of kink-like deformation bands in the prism. (a) Spatial orientation of the bands, after palaeomagnetic correction. (b) Histogram of angles between bands and bedding.

and 35%). They have only been noted in experiments on sediments with a water content greater than 30%. The kink-shear geometry mentioned above has also been seen by two of the authors in on-land sedimentary rocks, namely the Pliocene Emi Formation, South Boso Peninsula, Japan, and even these cemented rocks still have a porosity of around 30% (J. Ashi oral communication, 1991). It seems, therefore, that the kink- and shear zone-like-deformation bands reflect an early response to bulk prism shortening, particularly where it has become concentrated into localized horizons of high shear strain, and where the porosity of the sediments is still high.

Some fault-like bands may have evolved through excessive strain along shear zones, and the faults do seem to be promoted in zones of high localized strain. Indeed, their best development is within the zone of the frontal thrust, where they cross-cut other kinds of deformation bands, even where the latter have been rotated along with bedding to new orientations. There they clearly represent a separate, late stage of deformation, and in general the faults are thought to have originated independently of other deformation structures. Faults are more widespread spatially and chronologically, and require less restricted material properties. The faults probably represent intervals of high fluid pressure; during such periods, the reduced effective stress will have promoted inter-grain slippage, allowing high shear strains to be accomplished within very narrow zones of realigned, and geometrically softened, particles. The generally complex orientation patterns of the fault structures are thought to reflect a multiple and protracted faulting history in the prism.

Although deformation bands similar to those in the Nankai cores are now beginning to be recognized in onshore exposures, such as the Shimanto Belt—the Cretaceous precursor of the present Nankai structure (Taira *et al.* 1988), and the Pliocene rocks of the Miura

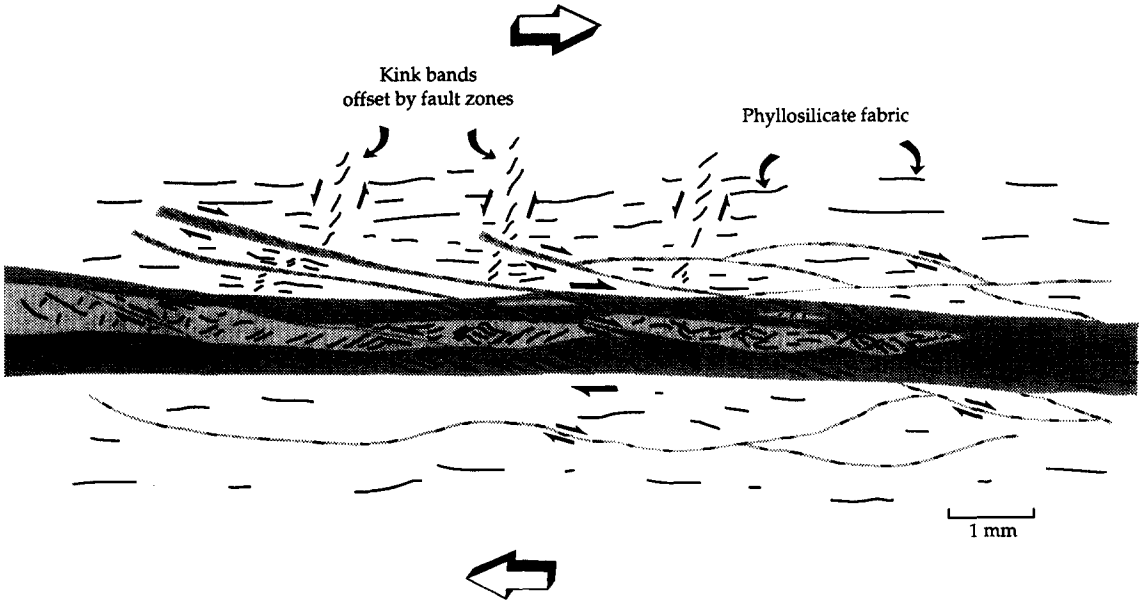

Fig. 8. Sketch of the microscopic appearance of a relatively thick fault zone from within the frontal thrust. Macroscopically the structure is irregular and black in colour like the structures shown in Fig. 5(d); microscopically, the structure shows intensely reoriented phyllosilicates with a complex substructure.

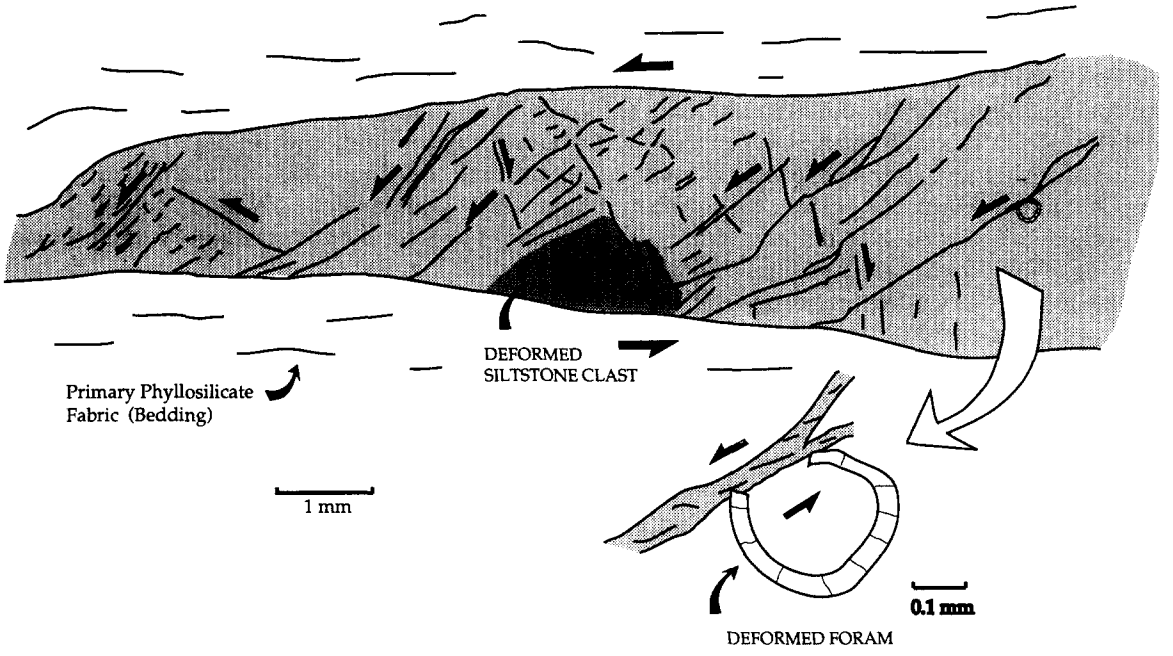

Fig. 9. Sketch of the microscopic appearance of a broad fault-like deformation band, showing the conjugate arrangement of sub-faults. 260 mbsf.

and Boso peninsulas (Ogawa & Taniguchi 1988), the extent to which these prism-toe features generally survive progressive accretion and uplift remains to be established.

Other structures

A number of horizons have undergone tectonic brecciation, and some include zones of shiny flakes and lensoid fragments resembling scaly clay. The brecciated horizons rarely exceed 1 m in thickness, except for the extensive development in the frontal thrust and basal décollement zones (Figs. 4a & d). The overall textures are similar to the shear fabrics well known in shale–matrix melange zones (e.g. Byrne 1984, Labaume *et al.* 1990). A breccia at 788 mbsf lacks fabric, and appears to have fragmented during *in situ* dilation (Fig. 5f). It is referred to here as a 'hydraulic breccia', and is thought to be due to localized overpressuring.

Vein structure occurs in several narrow bedding-parallel zones around 640 mbsf. Individual veins are slightly sigmoidal and approximately perpendicular to bedding. They comprise an abrupt but feeble realignment of coarser phyllosilicates exactly parallel to the vein margins (Fig. 5c), with finer particles retaining the orientation of the host material. The general appearance corresponds with the description given by Lundberg & Moore (1986).

Vein structure is being increasingly reported from convergent margins (e.g. Knipe 1986a,b, Lindsley-Griffin *et al.* 1990)—the striking feature about the Nankai examples is their scarcity. The few Nankai structures are closely similar in appearance to those discussed by Ogawa *et al.* (in press), who suggested that a certain combination of extensional stress, elevated pore-pressure and lithology was required for their formation. These conditions may have been achieved during deformation within the Nankai prism toe, for example on the outer arcs of thrust-related folds, but it is thought more likely that the vein structures formed before offscraping. Such an interpretation is strongly supported by the one record of vein structure from Leg 87—at Site 582, the reference hole oceanward of the prism. Interestingly enough, the depth of occurrence is almost identical to Site 808. Such structure is known to form in slope basin sediments extending through gravitational instability (Pickering *et al.* 1990, J. Ashi & Y. Ogawa oral communication, 1991), and the Nankai examples may well have a similar origin.

Fragments from the décollement that are coherent enough to examine microscopically show an unusual mottled texture. Diffusely-bounded, roughly oval patches, each containing a weak fabric aligned slightly differently from its neighbours, are in places separated by narrow discontinuous shear zones; they have proved impossible to photograph adequately. Despite this subtlety, the restriction of this singular texture to the décollement horizon may be signalling some genetic significance. Electron-microscopic examination of scaly shards from the décollement (Knipe *et al.* in preparation) has revealed an intricate arrangement of microbreccia pockets and collapsed phyllosilicate domains suggestive of a complex and protracted textural history (see overpressures, below).

DISTRIBUTION OF DEFORMATION WITH DEPTH

Upper prism

The distribution and orientation of deformation bands is depicted in Figs. 2 and 10. Clearly distinguish-

able faults are shown separately. Although the plot is thought to be a good representation of the real distribution of the structures, it is affected by the variable core recovery, particularly in the loose sediments at the shallow levels of the prism. Variation of bedding dip with depth is given in Fig. 2. The steepened and inverted bedding in the shallow horizons, together with some fold closures, are due to gravity-driven deformation.

The striking feature in the upper prism is the shallowness at which tectonic structures are forming. The sediments here are porous (>50%) and soft (shear strengths <200 kPa—easily cut with a cheese-knife), yet they contain deformation bands with all the characteristics of the deeper examples, and with orientations clearly demonstrating their tectonic origin. Complex examples of such structures were encountered at a mere 260 mbsf. The frontal thrust-fault itself outcrops on the ocean floor nearby. Moreover, the seismic profile (Moore *et al.* 1991) and a back-scattered sonar image (Taira *et al.* 1991b, p. 11) show the frontal thrust and numerous earlier, landward thrusts all reaching the ocean bottom. Clearly, tectonic stresses—by definition of deep-seated origin (Maltman in press)—can be readily transmitted through highly porous, wet sediments to shallow levels.

Frontal thrust zone

Deformation bands increase in intensity as the frontal thrust is approached, and faults become common. Within the thrust zone, kink-like deformation bands form complex arrays, but some have been rotated to retain their conjugate geometry about the now-steepened bedding, both features being abruptly cross-cut by intense faulting. Brecciation and scaly fabrics are also developed (Fig. 4a), making this, along with the basal décollement, one of the two most intensely deformed zones at Site 808.

Perhaps for this reason, core recovery in the thrust zone was relatively poor. Even so, it became possible to obtain considerable structural geological information. Sufficient bedding was detected, including some inverted graded-beds which also yielded inverted palaeomagnetic poles, to reconstruct the geometry of the zone (Fig. 3). Moreover, by combining the depth information from the two holes in which the thrust was cored with that from other holes in which a fractured zone was perceived from drilling characteristics (T. Pettigrew oral communication, 1990), and knowing the precise geographic locations of each hole, it was possible to calculate the real orientation of the thrust: 040/17SE. This dip value is lower than the 40° surmised from the seismic profile, and must represent a local variation; the structure may flatten to 15° near the ocean floor (Moore *et al.* 1991). On the basis of a 30° dip and the deformation seen in the cores, the true thickness of the frontal thrust zone (surface-perpendicular) is 26 m. A distinctive conglomerate horizon recognized both above and below the thrust serves as a displaced marker, yielding a stratigraphic throw of 146 m and, assuming a 30° dip for the structure, a fault-parallel separation of 309 m. This last value also represents the true movement so far accomplished by the thrust zone (i.e. the net slip), because slickenlines indicate a down-dip motion. The separation apparent in the plane of the seismic section from the displacement of a prominent reflector is close to this value, at 290 m (Moore *et al.* 1991).

Lower prism

The sediment in the lower part of the prism is partially lithified, in that it is difficult to cut with a knife and has to

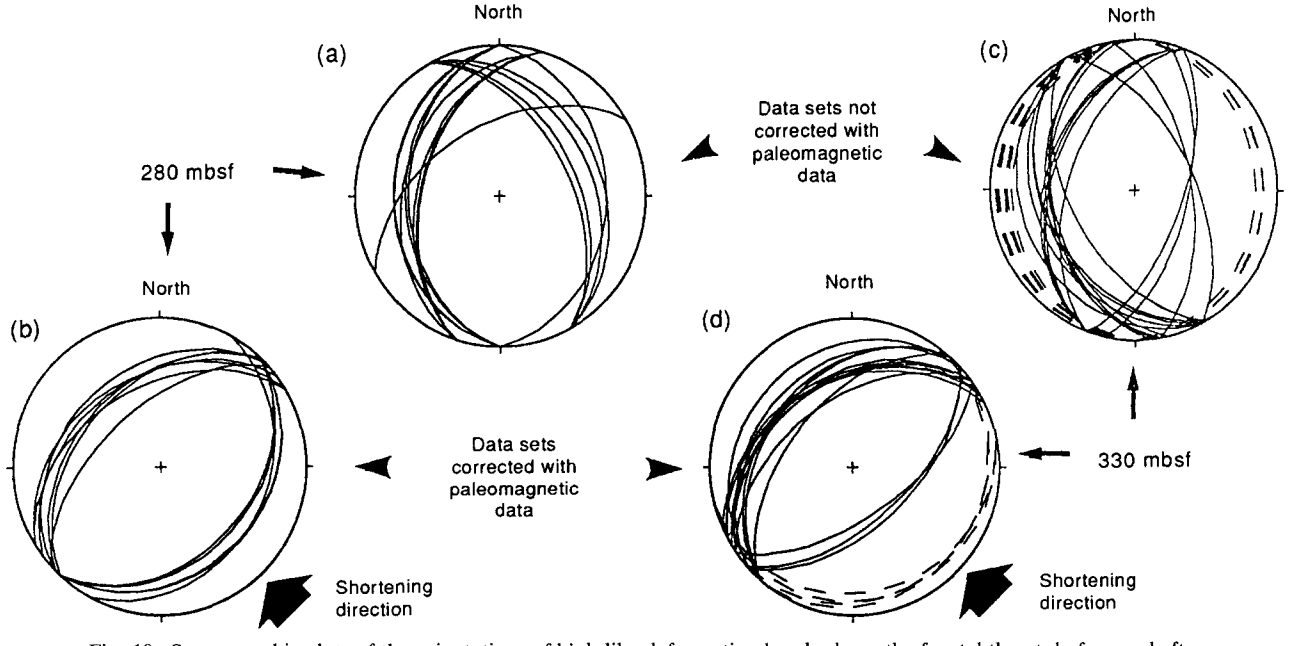

Fig. 10. Stereographic plots of the orientations of kink-like deformation bands above the frontal thrust, before and after palaeomagnetic correction for drilling rotations. The dashed lines in (c) and (d) are bedding; in (a) and (b) bedding is horizontal. Equal-area lower-hemisphere projections.

be sawn, but is still fragile and retains a porosity generally in excess of 35%. The distribution of deformation bands is inhomogeneous, but there is an overall decrease in intensity of developments of the kink- and shear zone-like features down to about 600 mbsf, below which fault-like structures dominate (Fig. 2). Horizons of more frequent bands, such as at 530–560 mbsf and around 800 mbsf, are regarded as localized zones of greater strain, an interpretation supported by the steepened bedding seen at these levels. These zones are thought to represent thrusts in their incipient stages. The 800 mbsf horizon also contains the hydraulic breccia and the sole sedimentary dyke, discussed further under overpressures, below.

Basal décollement

The basal décollement of the Nankai prism toe was encountered at about 945 mbsf. In the cores, the zone comprises intense brecciation and scaliness (Fig. 4d), a high concentration of faults, and marked increases in bedding dip (Fig. 2). Nevertheless it was possible to locate a 2 m section within the zone that is both structurally and magnetically coherent. Careful dissection of this material revealed that most faults dip towards the northwest and bear slickenlines that trend northwest, consistent with the kinematic results from within the prism and the direction of regional plate convergence.

The décollement shows three remarkable features. First, despite this structure being the critical junction between major global plates, the zone is no more that 19.2 m thick. (It could conceivably be as little as 12 m, depending on the precise depths to which the recovered core pieces are assigned.) Second, the zone is very sharply bounded. The top is marked by the abrupt onset of well-developed breccia, scaly fabric and increased faulting; the base is an almost knife-sharp change from very fine breccia to virtually undisturbed mudstone below. Third, because this lack of deformation immediately below the décollement continues at depth, the structure is separating materials of dramatically different deformation character. This contrast between the materials above and below the décollement is discussed further in the context of stress conditions. All the structural data confirm the seismic reflection images in pointing to the décollement zone as the most significant discontinuity in the toe region of the Nankai prism.

The underthrust sequence

The materials being underthrust beneath the prism are characterised by a paucity of deformation structures and essentially sub-horizontal bedding. Faults are sparse and show a variety of geometries, displacement senses and slickenline orientations—further emphasizing a stress history different from the prism. Some of the faults lack a dark filling and are considered to be of pre-accretion, possibly syn-sedimentary origin.

Vein structures occur at 1260 mbsf, but related to nearby layers of welded tuff rather than bulk dewatering processes. The shallowest veins (in the usual sense of mineralized fractures) observed at Site 808 are calcite-filled fractures from 1276 mbsf, in volcanic-rich hemipelagites of about 30% porosity. Further examples occur at 1282 mbsf, a sample that also contains fine, wavy stylolites (Fig. 5e). This location, about 316 m below the décollement and just 8 m above igneous basement, is the shallowest known example at Site 808 of diffusion mass transfer (pressure solution) having operated as a deformation mechanism.

The basaltic crust itself shows local zones of brecciation and various extensional veins of calcite and chlorite. These show no systematic organization and no slickenlined surfaces. These structures were probably developed from oceanic crustal processes and fluids circulating within the basalt rather than tectonism associated with the prism. The 363 m of underthrust material that was drilled is destined to be underplated or subducted, but has so far accomplished its journey below the continental plate with negligible deformation.

ROLE OF DEFORMATION IN PRISM DRAINAGE

Accreting sediments lose enormous amounts of water as they consolidate, especially in the toe regions of prisms (Bray & Karig 1985). In addition, fluids produced by mineral dehydration, hydrocarbon generation and from the oceanic crust, are being expelled. All this leads to a massive fluid flux through the prism to the seafloor (Moore 1989, Langseth & Moore 1990). It is not the present purpose to explore the ramifications of these major processes but some connections with structural geology are summarized below.

Channelized vs diffusive drainage

The locations and efficiencies of the drainage routes influence the overall prism deformation, and the resulting structures in turn influence the fluid flow pattern (Moore 1989). The success of ODP Leg 110 in identifying the role of tectonic structures as dewatering conduits (Moore *et al.* 1988, see also Langseth & Moore 1990 and following papers) led to the Barbados (Lesser Antilles) prism becoming something of a paradigm: the evidence from Leg 131 was widely expected to demonstrate that the Nankai prism, too, was undergoing channelized drainage (Fig. 11a).

However, the observations from Site 808 are ambiguous. In some ways the structural geological data are more comptabile with the Nankai prism draining pervasively rather than along discrete structures, although the interpretations are debatable. In contrast with the Barbados prism, neither the frontal thrust nor the décollement show any visible sign of channelized flow. For example, no mineralized veins are observed (Maltman *et al.* 1992), although this may reflect an inappropriate chemical environment rather than insufficient fluid flux. On the other hand, the palaeomagnetic and sonic anisotropy data indicate a pervasive tectonic consolidation of

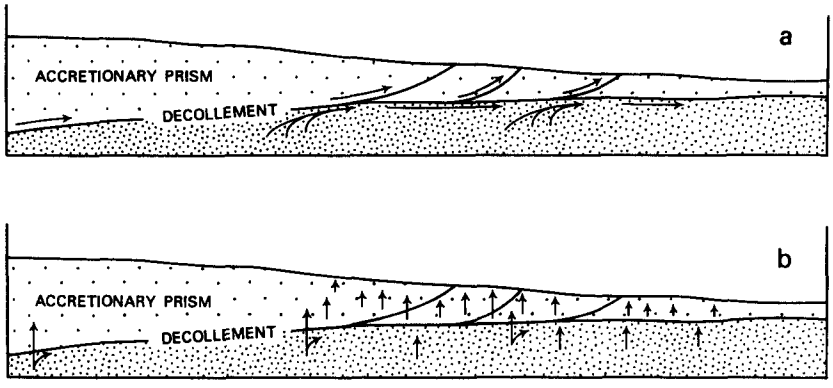

Fig. 11. Diagrams to show the difference between (a) channelized and (b) diffusive drainage of an accretionary prism.

the prism. It is possible that the unusually numerous deformation bands at Nankai may be aiding this diffuse drainage. CT X-ray scans indicate a greater sediment density within the bands, and although this may be partly due to porosity reduction, microprobe transects suggest that an Fe increase is also involved (Byrne *et al.* in preparation). Experimental work has documented fluid expulsion from such bands during their formation, followed by enhanced permeability along them (Arch & Maltman 1990). The Fe increase in the natural examples may therefore be reflecting this latter effect. Thermal and some geochemical evidence (Taira *et al.* in preparation) are also suggestive of a diffusive dewatering regime, although, on the other hand, a broad chloride anomaly at the décollement (Taira *et al.* 1991b) can be interpreted as recording localized flow. Thus the overall data are open to different interpretations, but in any event they do not fit readily with the Barbados model.

It may not be simply that prisms such as Nankai, dominated by clastic sediments, drain pervasively whereas clay-rich prisms such as Barbados develop conduits. There is some evidence that the flow regime at Nankai may be different along strike. Submersible-based observations of mud volcanos, biological communities, etc., suggest some channelized drainage in the NE Nankai Trough (e.g. Le Pichon 1991). Important strike-slip faults cross the Nankai prism transversely, and these may be dividing the prism into differing drainage regimes.

Evidence for overpressures in the prism

The influence of fluid pressures on prism dynamics is now well established (e.g. Moore 1989). In particular, the significance of overpressured horizons for localizing major discontinuities has been argued for prisms such as Barbados (e.g. Screaton *et al.* 1990), and would be expected to be a major effect at Nankai. The structural geological results from Leg 131: (1) support the interference of fluid pressures around the décollement zone; (2) indicate the existence of other localized horizons of overpressuring within the prism; but (3) are at best equivocal regarding the frontal thrust.

Regarding the décollement, electron-microstructural analysis of samples from the zone shows scaly films surrounding pockets of isotropic breccia. It seems that an episode of overpressuring produced brecciation, and was followed by strain softening and collapse to form the scaly domains. The sequence may be cyclic. The mottled texture seen at the optical microscope scale is also suspected to result, in a way not yet understood, from previous overpressuring. The increase in bulk density shown by the décollement (Fig. 2) implies that at present the structure is at a collapsed stage, perhaps sealing any transfer of fluids from below.

This latter idea is supported by one of the most dramatic observations to emerge from the Leg 131 drilling. The gradual decrease of porosity with burial in the prism accelerates slightly in the décollement, below which it shows an abrupt and striking increase (Fig. 2). Samples from immediately below the décollement show a sudden porosity increase in excess of 10%, a huge amount over such a narrow interval. These highly underconsolidated materials are almost certainly overpressured, presumably as a result of the sealing properties of the décollement. This is the clearest evidence at Site 808 for present-day overpressuring. Moreover, the seafloor sonar image about 12 km south of Site 808 (Taira *et al.* 1991b, p. 11) shows several mud volcanoes seaward from the frontal thrust, further substantiating that the underthrust sediments are overpressured.

In the uppermost 200 m of the prism, the great fluctuations in porosity (between 33 and 74%) are partly due to lithological variation and sample disturbance, but some of the positive deviations from a normal burial trend may be indicating very localized overpressuring. Indeed, at 186 mbsf excess fluid pressures were successfully measured *in situ*, for the first time in an accretionary setting (Taira *et al.* 1991a, p. 199). The pore pressure was about 4 MPa in excess of the 49 MPa hydrostatic value. That these sediments are overpressured is in line with the evidence of common gravitational instabilities observed at these surficial levels.

Deeper in the prism, those intervals showing increased bedding dip and deformation-band frequency are taken to represent horizons of enhanced shear strain, perhaps localized at sites of overpressuring and hence reduced sediment strength. These notions are well substantiated around 800 mbsf. In line with this being an anomalously high-strain zone, physical proper-

ties such as water content, acoustic velocity and impedance show an offset characteristic of a thrust fault (Taira *et al.* 1991b, p. 162). Substantiating the role of overpressuring is the presence here of the *in situ* 'hydraulic' breccia described earlier, and at 813 mbsf there occurs a 2 cm-wide clastic sandstone dyke—the only visible evidence in any of the Leg 131 cores for overpressuring.

The frontal thrust would also be expected to be utilising overpressured horizons, but no supporting evidence is forthcoming at Site 808. There is some offset of the porosity–depth trend (Fig. 2), but this is compatible with delayed dewatering due to recent or current thrust movement, bringing slightly more consolidated sediments over less dense material. Some geochemical arguments also suggest that the frontal thrust is a youthful or presently active feature, with little fluid activity. Structural geological observations provide no evidence for or against anomalous fluid pressures in the thrust zone.

Attempts to balance sections through the prism toe, in the manner common in fold-and-thrust belt studies, are complicated by these erratic and constantly evolving porosity distributions. It is clearly unreasonable here to assume constancy of volume. For example, the fold in the hangingwall of the frontal thrust (Fig. 1b) is presumably a ramp-related fault-bend anticline, but section balancing involving fixed bedding length and constant volume is no more than qualitatively successful (Moore *et al.* 1991, p. 17).

STRESS CONDITIONS IN THE PRISM

The distribution of the deformation bands (Fig. 2) discloses a marked heterogeneity in the intensity of the prism stress field, but the consistent NE strike of the majority of the structures, parallel to the trend of the Nankai trench, suggests a uniform stress orientation. Fault-plane and slickenline orientations have been used, through the method of Angelier (1990), to derive reduced stress tensors for the prism (Lallemant *et al.* in preparation). In general, σ_1 trends sub-horizontally towards the northwest—within a few degrees of the plate convergence vector. The principal stress axes shown in Fig. 12 have an azimuth around 314°: the convergence vector derived seismically by Seno (1977)

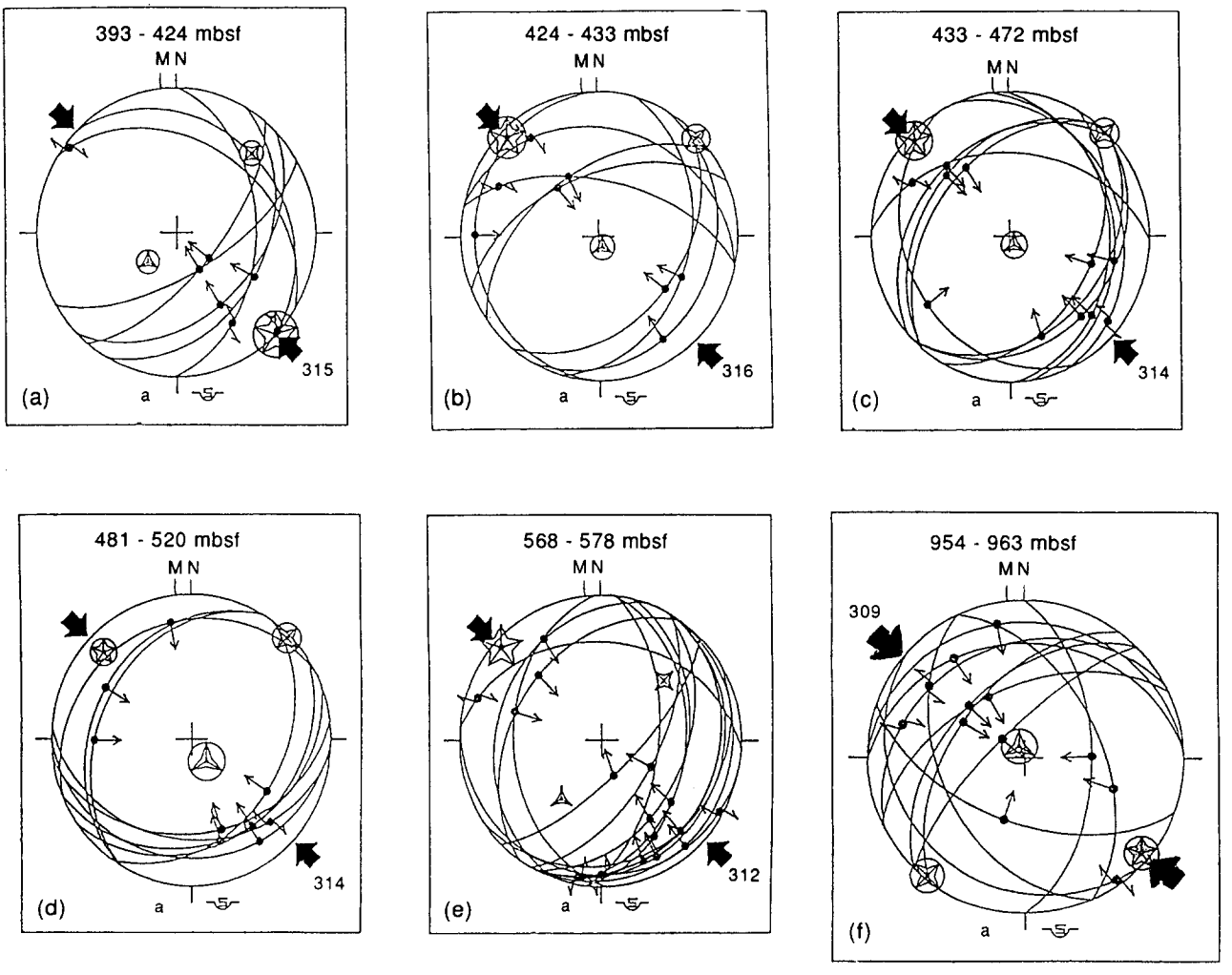

Fig. 12. Stereographic plots (lower-hemisphere projections) of fault orientations (great circles), slickenlines (dots) and reduced stress tensors from the lower prism. Depth ranges for each data set in mbsf are indicated. Plot (f) is from within the décollement zone. σ_1, σ_2 and σ_3 are shown with five-, four- and three-pointed stars, respectively, following the convention of Angelier (1990). Arrows pointing inwards and outwards denote slip directions for thrust and normal faults, respectively. Double arrows denote strike-slip motion. All of the data have been corrected palaeomagnetically for rotations due to drilling. See text for further discussion.

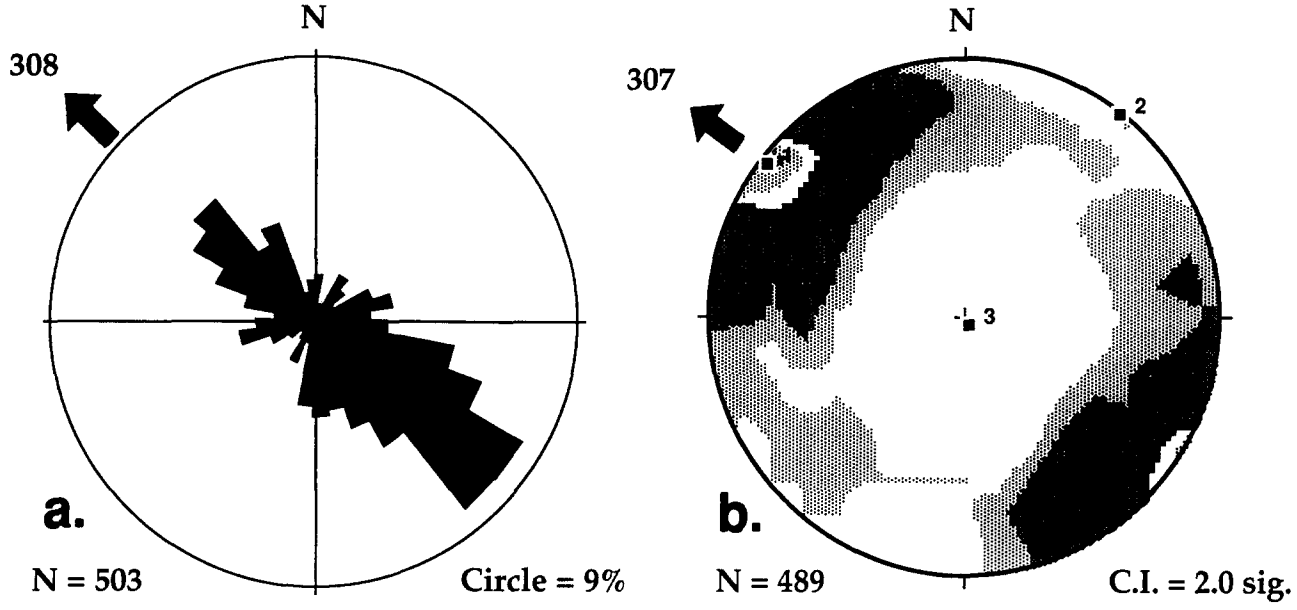

Fig. 13. Orientation data of all slickenline data. (a) Circular histogram form. (b) Stereographically as trends and plunges of incremental shortening axes, 1, 2 and 3 are the axes of greatest, median and least shortening, respectively.

was 310°, by Huchon (1986) 314° and by Ranken *et al.* (1984), 314°. The mean plunge is 3° NW, with the cone of 95% confidence extending only 5° around this. Such a shallow orientation is suggestive of a weak décollement, in line with the geophysical, physical properties and other structural data.

The reduced stress tensors derived from deeper in the prism are less clear, reflecting a more intricate faulting history (Lallemant *et al.* in preparation). A sequential history should tend to invalidate the stress tensor inversion results, and, arguably, the slickenline data would be better treated as incremental shortening axes (e.g Marrett & Allmendinger 1990). Figure 13 presents all the slickenline data collected, both as a circular histogram and stereographically as shortening axes. Mohr-diagram analysis of the best-fit stress tensors carried out by Lallemant *et al.* (in preparation) suggests that effective stress conditions varied significantly within the prism. The inverse analytical stress-technique has previously been restricted to fully lithified rocks, but the present work indicates its applicability to faulted unlithified sediments as well, although the capricious pore-pressures would hinder derivation of the complete stress tensor (Angelier 1989).

Physical properties such as magnetic susceptibility and horizontal acoustic anisotropy record a NW-oriented bulk shortening of the prism, which is presumably a response to the low-angle regional tectonic stresses. Leg 131 succeeded in measuring, for the first time in an active margin setting, lateral stresses *in situ*. Horizontal stresses of over 3.5 MPa, up to 1.9 times greater than that expected from burial alone, were measured at shallow levels at Site 808 (Taira *et al.* 1991a, p. 199 and fig. 152). Because many of the deeper sediments show significant overconsolidation, it is likely that lateral/vertical stress ratios are even greater deep in the prism.

All this is in dramatic contrast with the stress configuration below the prism. The underthrust sediments are conspicuously underconsolidated. Near to the décollement, where the burial stresses should normally be approximately 11 MPa, the effective burial load is estimated, on the basis of preliminary consolidation tests, to be no more than 3 MPa, implying a fluid pressure ratio (λ) about 0.9 (Karig in preparation). Moreover, the virtual absence of deformation structures below the décollement, together with the isotropy of the magnetic susceptibility and sonic velocities, indicate that the underthrust materials have undergone virtually no strain. They are tectonically and hydrologically isolated from the prism.

The question arises of how this decoupling is so effectively achieved by the décollement. It is not obvious how the zone can at the same time be dense enough to act as a drainage seal yet so overpressured and weak that none of the prism stresses are transferred across it. One explanation involves the laboratory-measured matrix densities not reflecting the significance of *in situ* fractures, in which fluid is trapped and overpressured. Another 'dynamic-seal', hypothesis has the horizontal fracture permeability so great and the the fluid stream issuing from the landward prism so energetic that drainage from below is prohibited (Moran *et al.* in preparation).

A different explanation involves a multiple behaviour. Until recently the décollement itself was highly overpressured and incapable of transmitting stress, but is now a temporarily dense seal, with any traction so far not significantly affecting the sediments below. The porosity and microstructural data are consistent with this. Moreover, there is evidence that the décollement is not currently accommodating a major part of the convergence strain. It was noted earlier that the frontal thrust is a youthful, probably active, feature. If the 0.02 Ma uppermost sediments (assuming constant sedimentation) are taken to be displaced about 300 m along a 30°-

dipping thrust, then, with a plate convergence rate of 40 mm a^{-1}, this single structure alone must have accommodated about 40% of the recent plate convergence. In addition, the other high-strain zones–incipient thrusts, and the pervasive prism shortening, account for further, as yet unquantified, proportions of the strain. Therefore, shear strain along the décollement today could be minor in comparison with recent times.

Whatever the exact mechanisms by which the décollement achieves its decoupling effect, the data make it clear that overpressuring is a crucial aspect. However, a fundamental matter on which Leg 131 has failed to shed light is an explanation for the location of the décollement. What caused the overpressuring in the particular horizon that was selected for décollement propagation? It is sited not, as might be expected, in the middle of a sedimentary section (Shi & Wang 1988) nor at the junction between the trench and hemipelagic deposits (Moore 1989, p. 97), but well within apparently uniform hemipelagites. The décollement protolith and the materials either side appear to consist of lithologically identical hemipelagic mud. Presumably some subtle property was sufficiently different in the selected horizon to have engendered at some stage a critically low permeability—but its nature remains to be discovered. Notwithstanding the wealth of data and the insights accumulated from Leg 131, questions about the early stages of accretion remain to be addressed by future drilling.

SUMMARY OF MAIN POINTS

(1) Gravity-driven deformation is important in the uppermost parts of the prism toe, probably due to overpressuring and local steepening of slopes. Accreted sediment slumps from rising hangingwall anticlines towards the trench, which may therefore contain a significant amount of recycled material.

(2) The tectonic stresses arising from plate convergence are being transmitted up through loose, wet sediments exceeding 50% porosity to high in the prism toe. Tectonically-induced deformation bands occur just 260 mbsf, and the frontal thrust of the prism, probably currently active, intersects the ocean floor. Techniques such as stress tensor inversion and section balancing, which are conventionally limited to rocks, can be applied to these poorly lithified materials, although capricious pore pressures and porosities cause difficulties.

(3) The frontal thrust, a 26 m thick zone of brecciated and scaly sediments containing a bedding fold-pair, has a net down-dip displacement of 309 m, equivalent to approximately 40% of the plate convergence of the most recent 20,000 years.

(4) Numerous core-scale deformation bands, varying in style between kinks, shear zones and faults, record different responses to bulk prism shortening. The structures are most numerous in and around the frontal thrust; other anomalous frequencies indicate horizons of high-strain, thought to be incipient thrusts. The faults are dominant in the deeper levels of the prism: below about 800 mbsf the sediments are insufficiently porous for the other kinds of bands to form.

(5) The basal décollement, encountered at 945 mbsf, consists chiefly of brecciated and scaly sediment similar to the frontal thrust. The zone is a mere 19 m thick, is very sharply bounded, and abruptly separates the tectonized prism sediments from virtually undeformed materials below.

(6) The 360 m of underthrust sediments show uniformly sub-horizontal bedding and a paucity of deformation features. The shallowest diffusion mass transfer known from this site is recorded by stylolites at 1200 mbsf (30% porosity), 8 m above the basaltic, oceanic basement.

(7) Vein structure is rare in the Nankai prism, and probably developed before offscraping. The scarcity of any kind of veining, relative to some other prisms, contrasts with the singular abundance of deformation structures in the Nankai cores.

(8) In further contrast with some other prisms, the structural geological evidence from Leg 131, in the central part of the Nankai prism, does not support a channelized drainage regime. In many ways, the observations are consistent with diffusive dewatering, but, overall, the interpretations are debatable. However, submersible-based observations in the northeast region of the prism, beyond some major strike-slip faults, point to a different pattern there. Accretionary prisms are more varied internally and differ more from each other than previously acknowledged.

(9) Fluid pressures are important for the prism structure. Overpressuring is documented from several deformed horizons within the prism, and exists today immediately below the décollement. No evidence for overpressures in the frontal thrust zone has been found.

(10) Stress tensor inversion based on striated fault planes in the prism sediments and within the décollement gives a principal compressive stress sub-horizontal towards the northwest, within a few degrees of the plate convergence vector. In contrast, the underthrust material is virtually undeformed.

(11) The tectonic and hydrological contrast between the prism and the underthrust materials is dramatic. However, debatable are the mechanisms by which the décollement becomes weak enough to accomplish the stress decoupling while remaining sufficiently dense to seal the sediments below.

(12) The lithology above, within, and below the décollement appears identical. Reasons for the location of the décollement horizon are unknown—an example of a problem remaining to be addressed by future drilling.

Acknowledgements—The improvements to the manuscript suggested by Casey Moore are gratefully acknowledged.

REFERENCES

Angelier, J. 1989. From orientation to magnitudes in paleostress determinations using fault slip data. *J. Struct. Geol.* **11**, 37–50.

Angelier, J. 1990. Inversion of field data in fault tectonics to obtain the regional stress. III—A new rapid direct inversion method by analytical means. *Geophys. J. Int.* **103,** 363–376.

Arch, J. & Maltman, A. J. 1990. Anisotropic permeability and tortuosity in deformed wet sediments. *J. geophys. Res.* **95,** 9035–9046.

Bray, C. J. & Karig, D. E. 1985. Porosity of sediments in accretionary prisms and some implications for dewatering processes. *J. geophys. Res.* **90,** 768–778.

Byrne, T. 1984. Early deformation in melange terranes of the Ghost Rocks Formation, Kodiak Islands, Alaska. In: *Melanges: Their Nature, Origin and Significance* (edited by Raymond, L. A.). *Spec. Pap. geol. Soc. Am.* **198,** 21–52.

Byrne, T., Bruckmann, W. & Owens, W. H. 1991. Correlation of core-scale structural fabrics, accoustic properties and magnetic anisotropy in an accreting sedimentary sequence (ODP Leg 131, Nankai Trough). *Trans. Am. Geophys. Un. (Eos)* **72,** 535.

Huchon, P. 1986. Comment on "Kinematics of the Phillipine Sea plate" by B. Ranken *et al. Tectonics* **5,** 165–168.

Karig, D. E. & Lundberg, N. 1990. Deformation bands from the toe of the Nankai accretionary prism. *J. geophys. Res.* **95,** 9099–9109.

Knipe, R. J. 1986a. Faulting mechanisms in slope sediments: examples from Deep Sea Drilling Project cores. In: *Structural Fabrics in Deep Sea Drilling Project Cores From Forearcs* (edited by Moore, J. C.). *Mem. geol. Soc. Am.* **166,** 45–54.

Knipe, R. J. 1986b. Microstructural evolution of vein arrays preserved in Deep Sea Drilling Project cores from the Japan Trench, Leg 57. In: *Structural Fabrics in Deep Sea Drilling Project Cores from Forearcs* (edited by Moore, J. C.). *Mem. geol. Soc. Am.* **166,** 75–87.

Labaume, P., Bousquet, J. C. & Lanzafame, G. 1990. Early deformation at a submarine compressive front: the Quaternary foredeep of Mt Etna, Sicily, Italy. *Tectonophysics* **177,** 349–366.

Langseth, M. G. & Moore, J. C., 1990. Introduction to special section on the role of fluids in sediment accretion, deformation, diagenesis, and metamorphism in subduction zones. *J. geophys. Res.* **95,** 8737–8741.

Le Pichon, X., Henry, P. & the Kaiko-Nankai Scientific Crew 1991. Implications of surface manifestations of fluids in subduction zones. *Phil. Trans. R. Soc.* **335,** 315–330.

Lindsley-Griffin, N., Kemp, A. & Swartz, J. F. 1990. Vein structures of the Peru margin, Leg 112. College Station, Texas (Ocean Drilling Program). *Proc. ODP, Sci. Results* **112,** 3–16.

Lundberg, N. & Karig, D. E. 1986. *Structural Features in Cores From the Nankai Trough, Deep Sea Drilling Project Leg 87A* (edited by Kagami, H., Karig, D. E., Coulbourn, W. T., *et al.*). *Init. Reps DSDP* **87,** 797–808.

Lundberg, N. & Moore, J. C. 1986. Macroscopic structural features in Deep Sea Drilling Project cores from forearc regions. In: *Structural Fabrics in Deep Sea Drilling Project Cores From Forearcs* (edited by Moore, J. C.). *Mem. geol. Soc. Am.* **166,** 13–44.

Maltman, A. J. 1978. Some microstructures of experimentally deformed argillaceous sediments. *Tectonophysics* **39,** 417–436.

Maltman, A. J. 1988. The importance of shear zones in naturally deformed wet sediments. *Tectonophysics* **145,** 163–175.

Maltman, A. J. In press. Prelithification deformation. In: *Continental Deformation* (edited by Hancock, P. L.). Pergamon Press, Oxford.

Maltman, A. J., Byrne, T., Karig, D. & Lallemant, S. 1992. Structural geological evidence from ODP Leg 131 regarding fluid flow in the Nankai prism, Japan. *Earth Planet. Sci. Lett.* **109,** 463–468.

Maltman, A. J., Byrne, T., Karig, D. & Lallemant, S. In press. Deformation structures at ODP Site 808, Nankai Accretionary Prism, Japan. *Proc. ODP, Sci. Results* **131.**

Mandl, G. 1988. *Mechanics of Tectonic Faulting.* Elsevier, Amsterdam.

Marrett, R. & Allmendinger, R. W. 1990. Kinematic analysis of fault-slip data. *J. Struct. Geol.* **12,** 973–986.

Moore, G. F., Karig, D. E., Shipley, T. H., Taira, A., Stoffa, P. L. & Wood, W. T. 1991. *Structural Framework of the Leg 131 Area, Nankai Trough* (edited by Taira, A., Hill, I. A. *et al.*). College Station, Texas (Ocean Drilling Program). *Proc. ODP, Init. Reps.* **131,** 15–23.

Moore, G. F., Shipley, T. H., Stoffa, P. L., Karig, D. E., Taira, A., Kuramoto, H., Tokuyama, H. & Suyehiro, K. 1990. Structure of the Nankai Trough accretionary zone from multichannel seismic reflection data. *J. geophys. Res.* **95,** 8753–8765.

Moore, J. C. 1989. Tectonics and hydrogeology of accretionary prisms: role of the décollement zone. *J. Struct. Geol.* **11,** 95–106.

Moore, J. C. & Lundberg, N. 1986. Tectonic overview of Deep Sea Drilling Project transects of forearcs. In: *Structural Fabrics in Deep Sea Drilling Project Cores From Forearcs* (edited by Moore, J. C.). *Mem. geol. Soc. Am.* **166,** 1–12.

Moore, J. C., Mascle, A., Taylor, E., Andreiff, P., Alvarez, F., Barnes, R., Beck, C., Behrmenn, J., Blanc, G., Brown, K., Clark, M., Dolan, J., Fischer, A., Gieskes, J., Hounslow, M., McClellan, P., Moran, K., Ogawa, Y., Sakai, T., Schoonmaker, J., Vrolijk, P., Wilkens, R. & Williams, C. 1988. Tectonics and hydrogeology of the northern Barbados ridge: results from ODP Leg 110. *Bull. geol. Soc. Am.* **100,** 1578–1593.

Ogawa, Y., Ashi, J. & Fujioka, K. In press. Vein structures and their tectonic implications for the development of the Izu-Bonin Forearc, ODP Leg 126. College Station, Texas (Ocean Drilling Program). *Proc. ODP, Sci. Results* **126.**

Ogawa, Y. & Taniguchi, H. 1988. Geology and tectonics of the Miura-Boso peninsulas and adjacent areas. *Modern Geol.* **12,** 147–168.

Pickering, K. T., Agar, S. M. & Prior, D. J. 1990. Vein structure and the role of pore fluids in early wet-sediment deformation, Late Miocene volcaniclastic rocks, Miura Group, SE Japan. In: *Deformation Mechanisms, Rheology and Tectonics* (edited by Knipe, R. J. & Rutter, E. H.). *Spec. Publs geol. Soc. Lond.* **54,** 417–430.

Rankin, B., Cardwell, R. K. & Karig, D. E. 1984. Kinematics of the Phillipine Sea plate. *Tectonics* **3,** 555–575.

Screaton, E. J., Wuthrich, D. R. & Dreiss, S. J. 1990. Permeabilities, fluid pressures, and flow rates in the Barbados Ridge Complex. *J. geophys. Res.* **95,** 8997–9007.

Seno, T. 1977. The instantaneous rotation vector of the Phillipine Sea plate relative to the Eurasia plate. *Tectonophysics* **42,** 209–226.

Shi, Y. & Wang, C.-Y. 1988. Generation of high pore pressures in accretionary prisms: Interferences from the Barbados subduction Complex. *J. geophys. Res.* **93,** 8893–8909.

Shimamoto, T. 1989. The origin of *S–C* mylonites and a new fault-zone model. *J. Struct. Geol.* **11,** 51–64.

Taira, A. *et al.* 1991a. College Station, Texas (Ocean Drilling Program). *Proc. ODP, Init. Reps* **131.**

Taira, A. *et al.* 1991b. A new thrust at accretion. *Nature* **347,** 228–229.

Taira, A., Katto, J., Tashiro, M., Okamura, M. & Kodama, K. 1988. The Shimanto Belt in Shikoku, Japan—evolution of Cretaceous to Miocene accretionary prism. *Modern Geol.* **12,** 5–46.

Taira, A., Tokuyama, H. & Soh, W. 1989. Accretion tectonics and evolution of Japan. In: *The Evolution of the Pacific Ocean Margins* (edited by Ben-Avraham, Z.). Oxford University Press, Oxford, 100–123.